 CMES, vol.76, no.1, pp.1-18, 2011

Numerical Solutions of 2-D Linear Elastostatic Problems by Network Method

J.L. Morales[1], J.A. Moreno[2] and F. Alhama[3]

Abstract: Following the rules of the network simulation method, a general purpose network model is designed and numerically solved for linear elastostatic problems formulated by the Navier equations. Coupled and nonlinear terms of the PDE, as well as boundary conditions, are easily implemented in the model by means of general purpose electrical devices named controlled current (or voltage) sources. The complete model is run in the commercial software PSPICE and the numerical results are post-processed by MATLAB to facilitate graphical representation. To demonstrate the reliability and efficiency of the proposed method two applications are presented: a cantilever loaded at one end and a supported loaded plate. Solutions are successfully compared with those provided by theoretical and standard numerical methods.

Keywords: Network Simulation Method, Linear Elasticity, Navier Equations.

Nomenclature

C_1	$(\lambda + 2\mu)$, (MPa)
C_2	μ, (MPa)
C_3	$(\lambda + \mu)$, (MPa)
E	Young's modulus, (MPa)
e	strain, (dimensionless)
f	body force, (N/mm^3)
F	force, (N)
i	electric current, (A)
gx, gy	controlled-voltage current-sources of the k-th cell of the circuits ux and uy, respectively, (A)
H	height, (mm)
L	length, (mm)

[1] Department of Structures and Construction, Technical University of Cartagena, Spain
[2] Department of Mechanical Engineering, Technical University of Cartagena, Spain
[3] Department of Applied Physics, Technical University of Cartagena, Spain

M	moment, (mm·N)
N	number of cells of the mesh grid
n	unit normal of S, (dimensionless)
q	load, (N/mm)
R	electric resistor, (Ω)
S	body's surface
t	traction prescribed over the surface S_t, (MPa)
V	electric voltage, (V)
u	displacement, (mm)
ux, uy	voltages at the circuit ux (eq. 19) or uy (eq. 20)
δ_{ij}	Kronecker delta
λ	Lamé's constant, (MPa)
μ	shear modulus, (MPa)
ν	Poisson's ratio, (dimensionless)
σ	stress, (MPa)
Ω	domain of the body
Δx, Δy	horizontal and vertical size of the cell, (mm)

Subscripts

,	according to the index notation, the comma in the subscript indicates the derivative with respect to the variables following it, while repeated indices imply summation over the range of indices, e.g. $u_{i,j} = \frac{\partial u_i}{\partial x_j}$, $e_{kk} = e_{11} + e_{22} + e_{33}$
i, j, k	vector components (i , j , k = 1 , 2 , 3)
ij	tensor components
x, y, z	rectangular components
k,0; k,1; k,2; k,3 and k,4	central, bottom, right, top and left locations of the k-th cell (Fig. 3)
kr,0; kr,1; kr,2; kr,3 and kr,4	idem at the right k-th cell
kl,0; kl,1; kl,2; kl,3 and kl,4	idem at the left k-th cell
kt,0; kt,1; kt,2; kt,3 and kt,4	idem at the upper k-th cell
kb,0; kb,1; kb,2; kb,3 and kb,4	idem at the lower k-th cell
t, u	referring to traction or displacement

Superscripts

b	prescribed function (displacement or traction) at the boundary surface

1 Introduction

Navier's linear elasticity equations generally require numerical solutions even in the case of simple geometries. This is mainly due to their inherent complexity since they contain coupling terms. Furthermore, the application of boundary conditions is not exempt of difficulty. In this paper we present a new tool for the numerical solution of this kind of problem based on the Network simulation method [González (2002)], a technique that has been applied in many other fields of engineering and science, including heat transfer, tribology, electrochemical, transport through membranes, fluid flow with solute transport in porous media, inverse problems, etc., reflecting its efficiency and reliability [Horno, González-Caballero, Hayas and González-Fernández (1990); Horno, Garcia-Hernández and González-Fernández (1993); Moreno, Gómez de León Hyjes and Alhama (2007); Soto, Alhama and González-Fernández(2007); Zueco and Alhama, (2007)].

The design of a network model for an elementary cell or finite volume starts with the finite-difference equations that result from the spatial discretization of the linear elasticity PDE. Whatever their form in so far as the mathematical dependence between dependent and independent variables is concerned, the terms of each equation are implemented separately in the model by a component whose constitutive equation is just such a dependence; in turn, the electrical component is connected to those related with the other terms of the equation depending on its topology. The components, such as controlled current (or voltage) sources, contained in most libraries of the electric simulation software are able to implement any kind of nonlinearity contained in the mathematical model and related either with the material or with the boundary conditions.

There are as many electric components as there are addends in each equation, and as many networks (or independent circuits) as there are finite-difference equations. Once the network model of the cell has been designed, it is electrically connected to the rest of the cells to complete the model of the whole geometrical domain. Finally, boundary and initial conditions must also be implemented by means of suitable electric components. The whole model is run on circuit simulation software, such as PSPICE [Microsim Corporation (1994); Nagel (1977)], which provides the numerical solution of the network without the need for any other mathematical manipulation by the user. A MATLAB subroutine reads the output data files of the simulation created by PSPICE before post-processing and representing these data (stresses and displacements) by appropriate 2-D and 3-D graphics. Errors only occur in the number of volume elements chosen for the discretization, and can be reduced to approximately 1% when the mesh grid is of the order of 50×50, or larger in 2-D square geometry problems.

After presentation of the linear elasticity equations and of details concerning the design of the model (sections 'governing equations' and 'design of the network model', respectively), two applications are solved to demonstrate the efficiency and reliability of the proposed model: the bending of an end-loaded cantilever (two cases, one loaded at the free end with a moment and the other with a shear force) and a simply supported loaded plate (also two cases, uniform and non-uniform load). Comparisons with theoretical and numerical (FEM) solutions are made in all cases.

2 Governing equations

Using the strain-displacement equations, $e_{ij} = \frac{1}{2}(u_{i,j} + u_{j,i})$, and the generalized form of Hooke's law for linear isotropic solids, $\sigma_{ij} = \lambda e_{kk}\delta_{ij} + 2\mu e_{ij}$, the equilibrium equations, $\sigma_{ij,j} + f_i = 0$, can be written in terms of the displacements as [Sadd (2009)]

$$(\lambda + \mu)\, u_{k,ki} + \mu u_{i,kk} + f_i = 0 \tag{1}$$

Eq.1 is named the Navier or Lame equation for the static problem in linear isotropic solids with uniform temperature and prescribed body force distribution f_i. For rectangular coordinates, Eq.1 is broken down into three scalar equations

$$(\lambda + \mu)\frac{\partial}{\partial \mathrm{x}}\left(\frac{\partial u_x}{\partial \mathrm{x}} + \frac{\partial u_y}{\partial \mathrm{y}} + \frac{\partial u_z}{\partial \mathrm{z}}\right) + \mu\left(\frac{\partial^2 u_x}{\partial \mathrm{x}^2} + \frac{\partial^2 u_x}{\partial \mathrm{y}^2} + \frac{\partial^2 u_x}{\partial \mathrm{z}^2}\right) + f_x = 0 \tag{2}$$

$$(\lambda + \mu)\frac{\partial}{\partial \mathrm{y}}\left(\frac{\partial u_x}{\partial \mathrm{x}} + \frac{\partial u_y}{\partial \mathrm{y}} + \frac{\partial u_z}{\partial \mathrm{z}}\right) + \mu\left(\frac{\partial^2 u_y}{\partial \mathrm{x}^2} + \frac{\partial^2 u_y}{\partial \mathrm{y}^2} + \frac{\partial^2 u_y}{\partial \mathrm{z}^2}\right) + f_y = 0 \tag{3}$$

$$(\lambda + \mu)\frac{\partial}{\partial \mathrm{z}}\left(\frac{\partial u_x}{\partial \mathrm{x}} + \frac{\partial u_y}{\partial \mathrm{y}} + \frac{\partial u_z}{\partial \mathrm{z}}\right) + \mu\left(\frac{\partial^2 u_z}{\partial \mathrm{x}^2} + \frac{\partial^2 u_z}{\partial \mathrm{y}^2} + \frac{\partial^2 u_z}{\partial \mathrm{z}^2}\right) + f_z = 0 \tag{4}$$

Boundary conditions can be formulated in displacement or in traction terms, as

$$u_i = u_i^b \text{ on } S_u \tag{5}$$

$$\sigma_{ij} n_j = t_i^b \text{ on } S_t \tag{6}$$

S_u denotes boundary surface points where the displacement values u_i^b are prescribed, while S_t refers to points where the traction values t_i^b are also given. Note that $S = S_t + S_u$ represents the complete boundary surface, Fig. 1.

Substituting Hooke's law in terms of the displacements, $\sigma_{ij} = \lambda u_{k,k}\delta_{ij} + \mu(u_{i,j} + u_{j,i})$, in Eq.6, the last equation can be written as a function of the displacement

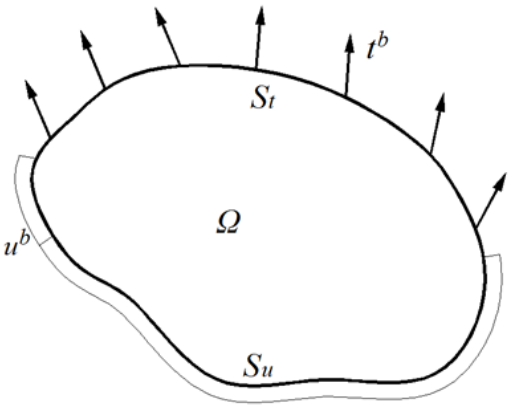

Figure 1: Scheme of the boundary conditions: tractions and displacements

variables [Timoshenko and Goodier (1951)] as

$$t_x^b = \lambda\left(\frac{\partial u_x}{\partial \mathrm{x}}+\frac{\partial u_y}{\partial \mathrm{y}}+\frac{\partial u_z}{\partial \mathrm{z}}\right)n_x+\mu\left(\frac{\partial u_x}{\partial \mathrm{x}}n_x+\frac{\partial u_x}{\partial \mathrm{y}}n_y+\frac{\partial u_x}{\partial \mathrm{z}}n_z\right) + \mu\left(\frac{\partial u_x}{\partial \mathrm{x}}n_x+\frac{\partial u_y}{\partial \mathrm{x}}n_y+\frac{\partial u_z}{\partial \mathrm{x}}n_z\right) \quad (7)$$

$$t_y^b = \lambda\left(\frac{\partial u_x}{\partial \mathrm{x}}+\frac{\partial u_y}{\partial \mathrm{y}}+\frac{\partial u_z}{\partial \mathrm{z}}\right)n_y+\mu\left(\frac{\partial u_y}{\partial \mathrm{x}}n_x+\frac{\partial u_y}{\partial \mathrm{y}}n_y+\frac{\partial u_y}{\partial \mathrm{z}}n_z\right) + \mu\left(\frac{\partial u_x}{\partial \mathrm{y}}n_x+\frac{\partial u_y}{\partial \mathrm{y}}n_y+\frac{\partial u_z}{\partial \mathrm{y}}n_z\right) \quad (8)$$

$$t_z^b = \lambda\left(\frac{\partial u_x}{\partial \mathrm{x}}+\frac{\partial u_y}{\partial \mathrm{y}}+\frac{\partial u_z}{\partial \mathrm{z}}\right)n_z+\mu\left(\frac{\partial u_z}{\partial \mathrm{x}}n_x+\frac{\partial u_z}{\partial \mathrm{y}}n_y+\frac{\partial u_z}{\partial \mathrm{z}}n_z\right) + \mu\left(\frac{\partial u_x}{\partial \mathrm{z}}n_x+\frac{\partial u_y}{\partial \mathrm{z}}n_y+\frac{\partial u_z}{\partial \mathrm{z}}n_z\right) \quad (9)$$

Finally, for 2-D plane strain (Fig. 2), Eqs. 2-9 reduce to

$$(\lambda+\mu)\frac{\partial}{\partial \mathrm{x}}\left(\frac{\partial u_x}{\partial \mathrm{x}}+\frac{\partial u_y}{\partial \mathrm{y}}\right)+\mu\left(\frac{\partial^2 u_x}{\partial \mathrm{x}^2}+\frac{\partial^2 u_x}{\partial \mathrm{y}^2}\right)+f_x=0 \quad (10)$$

$$(\lambda+\mu)\frac{\partial}{\partial \mathrm{y}}\left(\frac{\partial u_x}{\partial \mathrm{x}}+\frac{\partial u_y}{\partial \mathrm{y}}\right)+\mu\left(\frac{\partial^2 u_y}{\partial \mathrm{x}^2}+\frac{\partial^2 u_y}{\partial \mathrm{y}^2}\right)+f_y=0 \quad (11)$$

$$u_x = u_x^b, \quad u_y = u_y^b \text{ on } S_u \tag{12}$$

$$t_x^b = \lambda \left(\frac{\partial u_x}{\partial \mathrm{x}} + \frac{\partial u_y}{\partial \mathrm{y}} \right) n_x + \mu \left(\frac{\partial u_x}{\partial \mathrm{x}} n_x + \frac{\partial u_x}{\partial \mathrm{y}} n_y \right) + \mu \left(\frac{\partial u_x}{\partial \mathrm{x}} n_x + \frac{\partial u_y}{\partial \mathrm{x}} n_y \right) \text{ on } S_t \tag{13}$$

while for 2-D plane stress the Eqs.2-4 yield

$$\frac{E}{2(1-\nu)} \frac{\partial}{\partial \mathrm{x}} \left(\frac{\partial u_x}{\partial \mathrm{x}} + \frac{\partial u_y}{\partial \mathrm{y}} \right) + \mu \left(\frac{\partial^2 u_x}{\partial \mathrm{x}^2} + \frac{\partial^2 u_x}{\partial \mathrm{y}^2} \right) + f_x = 0 \tag{14}$$

$$\frac{E}{2(1-\nu)} \frac{\partial}{\partial \mathrm{y}} \left(\frac{\partial u_x}{\partial \mathrm{x}} + \frac{\partial u_y}{\partial \mathrm{y}} \right) + \mu \left(\frac{\partial^2 u_y}{\partial \mathrm{x}^2} + \frac{\partial^2 u_y}{\partial \mathrm{y}^2} \right) + f_y = 0 \tag{15}$$

with boundary conditions similar to those of the plane strain formulation (Eqs.12-14).

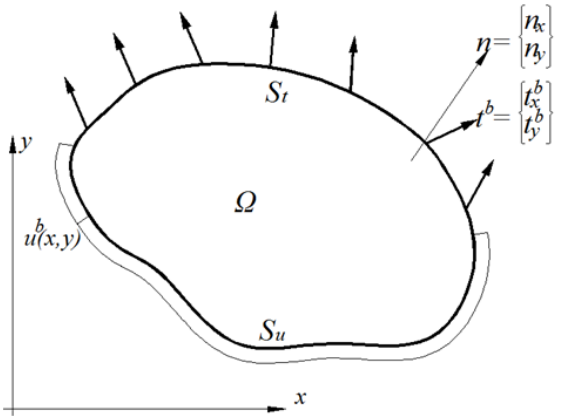

Figure 2: 2-D boundary conditions formulated by traction or displacement variables

Note that the plane stress problem can be expressed with the same equations as the plane strain case, replacing $\lambda = \frac{\nu E}{(1+\nu)(1-2\nu)}$ by $\lambda' = \frac{\nu E}{(1-\nu^2)}$ (Sadd, 2009).

In short, the solution of both 2D problems (plane stress and plane strain) using the displacement formulation involves determination of the plane's displacements (u_x,, u_y) in Ω, while the PDE (Eqs.10-11) is solved with the boundary conditions (Eqs.12-14).

3 Design of the network model

For a greater convenience, we shall group Eqs.10-11 in the form

$$(\lambda+2\mu)\frac{\partial^2 u_x}{\partial x^2}+\mu\frac{\partial^2 u_x}{\partial y^2}+\left[(\lambda+\mu)\frac{\partial^2 u_y}{\partial x\partial y}+f_x\right]=0 \tag{16}$$

$$\mu\frac{\partial^2 u_y}{\partial x^2}+(\lambda+2\mu)\frac{\partial^2 u_y}{\partial y^2}+\left[(\lambda+\mu)\frac{\partial^2 u_x}{\partial x\partial y}+f_y\right]=0 \tag{17}$$

Now, using the nomenclature of Fig. 3 for the discretized spatial variables, these equations change to finite-difference equations:

$$\frac{ux_{k,0}-ux_{k,2}}{(\triangle x^2/2)\frac{1}{C_1}}+\frac{ux_{k,0}-ux_{k,4}}{(\triangle x^2/2)\frac{1}{C_1}}+\frac{ux_{k,0}-ux_{k,3}}{(\triangle y^2/2)\frac{1}{C_2}}+\frac{ux_{k,0}-ux_{k,1}}{(\triangle y^2/2)\frac{1}{C_2}}$$
$$-\left[\frac{uy_{kt,2}-uy_{kt,4}-uy_{kb,2}+uy_{kb,4}}{2\triangle x\triangle y\frac{1}{C_3}}+f_x\right]=0 \tag{18}$$

$$\frac{uy_{k,0}-uy_{k,2}}{(\triangle x^2/2)\frac{1}{C_2}}+\frac{uy_{k,0}-uy_{k,4}}{(\triangle x^2/2)\frac{1}{C_2}}+\frac{uy_{k,0}-uy_{k,3}}{(\triangle y^2/2)\frac{1}{C_1}}+\frac{uy_{k,0}-uy_{k,1}}{(\triangle y^2/2)\frac{1}{C_1}}$$
$$-\left[\frac{ux_{kt,2}-ux_{kt,4}-ux_{kb,2}+ux_{kb,4}}{2\triangle x\triangle y\frac{1}{C_3}}+f_y\right]=0 \tag{19}$$

In these equations, the coefficients C_1, C_2 and C_3 are defined as $C_1=(\lambda+2\mu)$, $C_2=\mu$ and $C_3=(\lambda+\mu)$ for plane strain and $C_1=(\lambda'+2\mu)$, $C_2=\mu$, $C_3=(\lambda'+\mu)$ for plane stress.

Now, we shall define the formal equivalence between mechanical (displacement) and electric (voltage) variables, u and V, respectively. On the one hand, the first four addends of Eq.19 and Eq.20 can be assumed to be electric current through branches formed by simple resistors since the constitutive relations of these passive components are of the form i = ΔV/R. The branches of each circuit – as mentioned above, each equation refers to a separate circuit – meet at a common node according to the sign of the addend, Fig. 4. On the other hand, the last addend (between brackets in Eqs.19-20) is also assumed as a fifth current flowing out of the node – note that these addends represent the coupled term of the governing equations. These currents are implemented with a device known as a controlled current source, which provides a variable current that can be defined as an arbitrary, continuous function of the voltages at any node of the two networks. The specification of this current is easily introduced by software following simple programming rules.

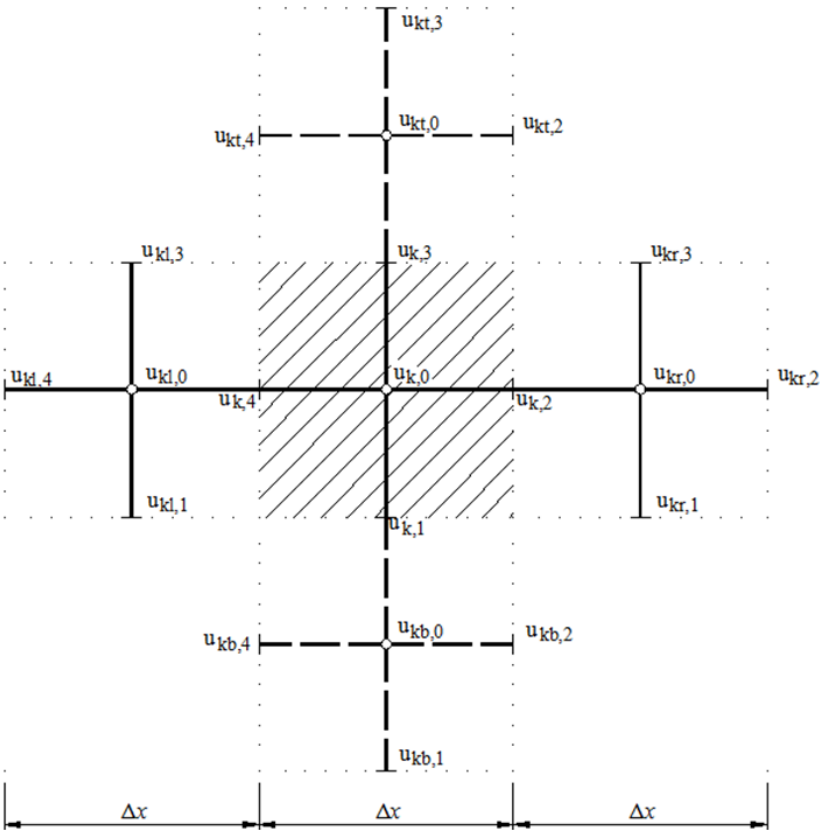

Figure 3: Nomenclature of the nodes for the network. Note that there is one figure for the ux and another figure for the uy circuit

To complete the model of the whole domain, $N_x \times N_y$ networks must be electrically connected to each other along axes x and y, Fig. 3. It is important to mention that volume elements do not necessarily need to have a square geometry, and they can be rectangular, irregular parallelograms and even triangular or slightly curvilinear [Moreno, Gómez de León Hyjes and Alhama (2007)]. This approximation allows the mesh to be improved for better adaptation to the particular geometry of the problem.

Finally, displacement boundary conditions, Eq.12, are directly implemented by means of constant voltage generators, while traction conditions, Eqs.13-14, are implemented by controlled voltage sources. For example, for the case $n_x = 0$ and

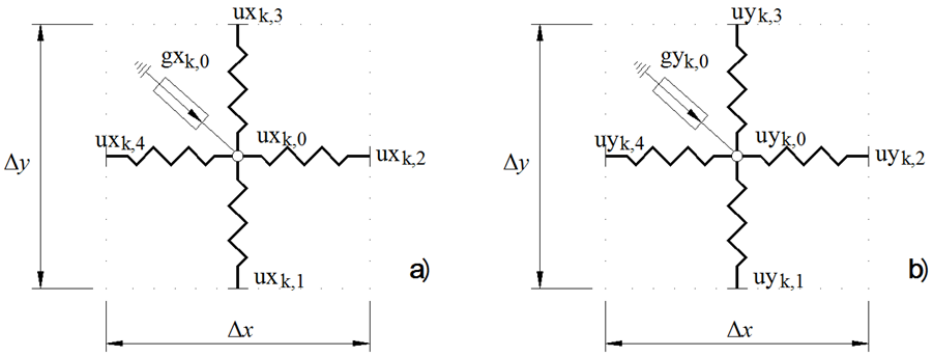

Figure 4: Network model of the volume element: a) Circuit ux. b) Circuit uy

$n_y = 1$ (Fig. 5), boundary conditions simplify to

$$t_x^b = \mu \left(\frac{\partial u_x}{\partial y} + \frac{\partial u_y}{\partial x} \right) \tag{20}$$

$$t_y^b = \lambda \frac{\partial u_x}{\partial x} + (\lambda + 2\mu) \frac{\partial u_y}{\partial y} \tag{21}$$

Now, taking finite difference for the spatial variables, the displacements (voltage sources) are yielded

$$ux_{k,3} = ux_{k,0} + \frac{\triangle y}{2} \frac{t_x^b|_{k,3}}{\mu} - \frac{\triangle y}{4\triangle x} \left(uy_{kr,3} - uy_{kl,3} \right) \tag{22}$$

$$uy_{k,3} = uy_{k,0} - \frac{\triangle y}{2(\lambda + 2\mu)} \left[-t_y^b|_{k,3} + \frac{\lambda}{2\Delta x} \left(ux_{kr,3} - ux_{kl,3} \right) \right] \tag{23}$$

Once the network model is completed, it is run on suitable circuit simulation software such as PSPICE. There are two ways to do this: direct introduction, following the electric scheme in the 'schematics' ambient of the software, or by creating a network text file. In both cases, very few programming rules are necessary since only three electric components are contained in the network: resistors and controlled current or voltage sources.

The advantages of the network method are several. Firstly, once the model has been designed, it is easily introduced in the network simulation code with no other mathematical manipulations of the user; everything is done by the software. In addition, modern codes implement the most sophisticated and powerful mathematical algorithms which are able to simulate extremely non-linear signals, providing the exact

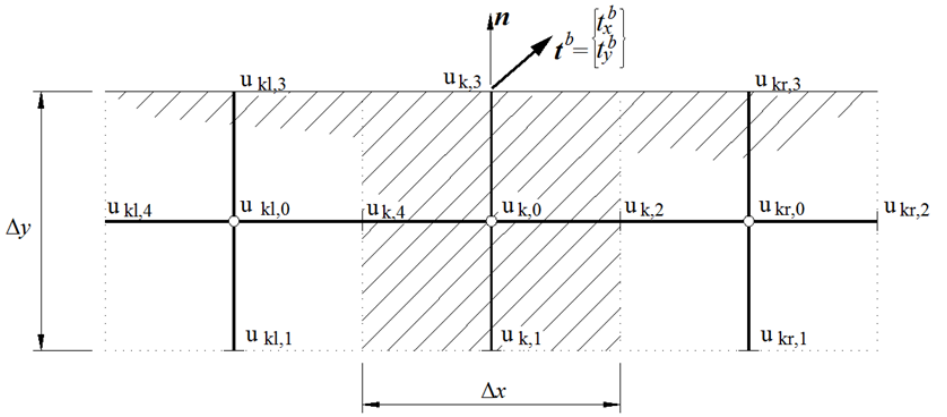

Figure 5: Boundary conditions. Traction at the surface coordinate ($n_x = 0$, $n_y = 1$). Note that there is one figure for the ux and another figure for the uy circuit

solution of the network (errors are only due to the size of the mesh grid). Besides, the code (PSPICE) suitably modifies the time step of the simulation according to the smoothness of the solution in order to reduce the computational times.

Although PSPICE has its own output graph ambient to show the 1-D simulation results, the output data files generated by the simulation are read and processed by MATLAB using a programming routine created to this end. This routine permits 2-D and 3-D graphics of the solution to be represented. Total computing time (simulation and post-processed) for the proposed applications is negligible, less than 10 s.

4 Application examples

4.1 Application 1: Cantilever loaded at the end

4.1.1 Case a: Loaded at the free end with a moment M (pure bending)

Consider the plane stress problem of an isotropic elastic cantilever under bending load, with zero body forces. The dimensions and boundary conditions are shown in Fig. 6. The geometrical parameters are: L = 200 mm, H = 100 mm and thickness = 10 mm, while elastic constants are $E = 210$ GPa and $\nu = 0.3$. The moment on the free end is M = 4E6 mmN and the grid size $N_x = 62$, $N_y = 31$. This problem was studied by Timoshenko and Goodier (1951), who assumed a linear force distribution to represent the moment imposed by the boundary condition at the free end of the cantilever.

Vertical displacements at $y = 0$ (deflection curve) provided by the simulation are shown in Fig. 7, while stress σ_{xx} (bending stress) along the cross section at $x =$ 150 mm is represented in Fig. 8. In these figures, theoretical displacements and stresses are also represented for comparison purposes. As can be seen, the results are nearly the same. A detail of the displacement and stress results, using five significant digits, for point A (centroid of the free end cross section) and B (a target point of the free surface), respectively, as well as their negligible errors, is shown in Tab. 1.

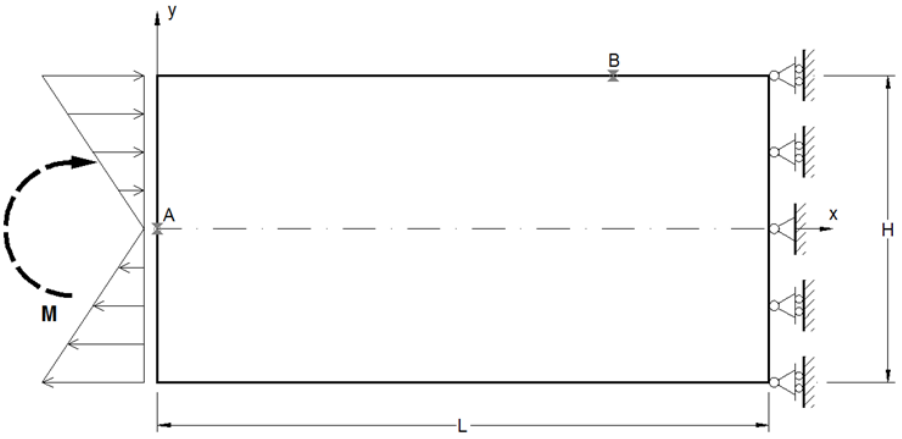

Figure 6: Geometry and boundary conditions. Application 1, case a

Table 1: Comparison between network and theoretical solutions [Timoshenko and Goodier (1951)]. Application 1, case a

	Theoretical	Network	Ratio	Error (%)
Point A: Deflection $u_{y,}$ (mm)	0.45714	0.45673	0.9991	0.09
Point B: Stress σ_{xx}, (MPa)	-240.00	-239.72	0.9988	0.12

4.1.2 Case b: Loaded at the free end with a force F

This problem is inspired by a theoretical case studied by Timoshenko and Goodier (1951), who solves it for an ideal mathematical boundary condition at the fixed end, which is not a typical condition in standard numerical codes. The dimensions and boundary conditions are shown in Fig. 9. The shearing force on the free end, F =

20E3 N, is distributed according to the parabolic law given in the classical books on the strength of materials [Timoshenko and Goodier (1951)]. Points belonging to the right end are assumed fixed. The geometrical parameters, material properties and grid size are similar to the case described above (case a).

Figs. 10 and 11 show the stress and displacement isolines, σ_{xx} and u_x, respectively, provided by network and FEM solutions for comparison purposes. For the latter,

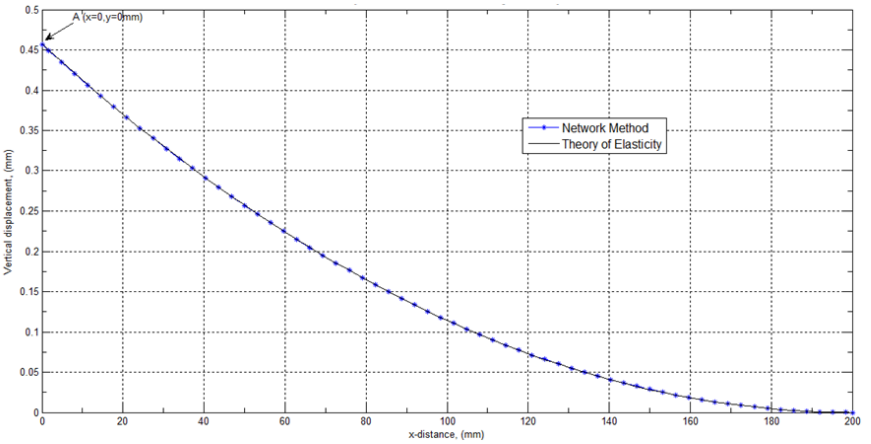

Figure 7: Vertical displacements results at $y = 0$. Application 1, case a

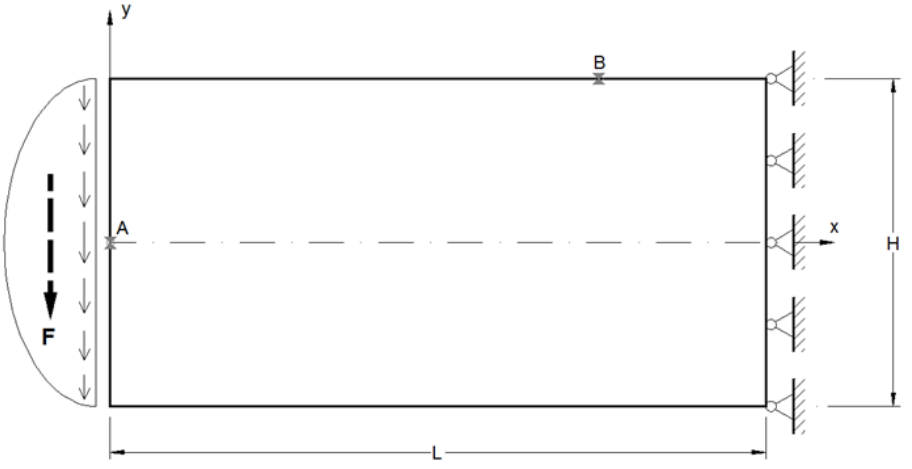

Figure 10: Geometry and boundary conditions. Application 1, case b

a 2-D structural solid element, which is defined by four nodes with two degrees of freedom at each node [ANSYS 9.0 (2004)], and a grid size 60×30 was used. As in the above case, a detail of these close results is presented in the Table 2.

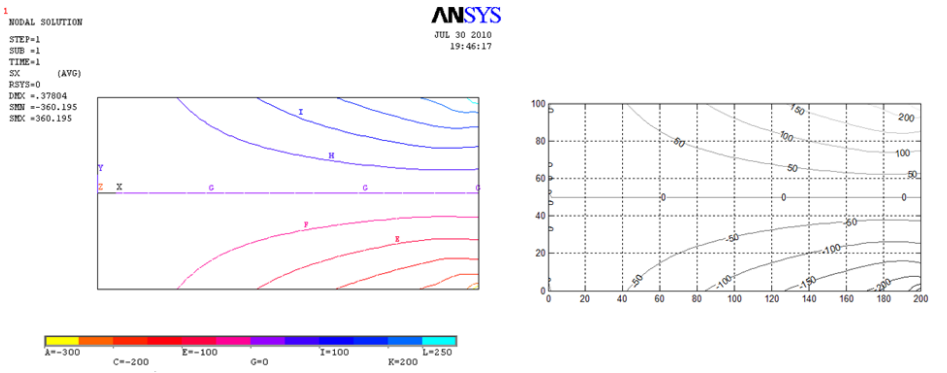

Figure 11: Stress Isolines, σ_{xx}. Left: FEM solution, right : Network solution. Application 1, case b

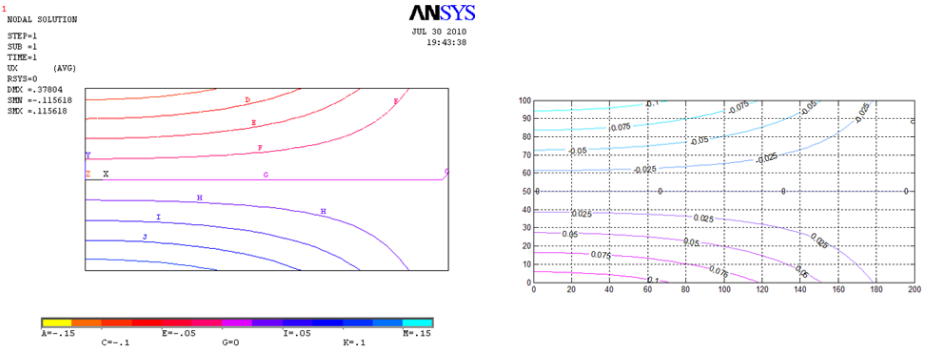

Figure 12: Displacement isolines u_x. Left: FEM solution, right : Network solution. Application 1, case b

Table 2: Comparison between network and FEM solutions. Application 1, case b

	FEM	Network	Ratio	Deviation(%)
Point A: Deflection u_y, (mm)	-0.35995	-0.35620	0.9896	1.04
Point B: Stress σ_{xx}, (MPa)	+179.45	+177.07	0.9867	1.33

4.2 Application 2: Simply supported loaded plate

4.2.1 Case a. Bending by uniform load

This considers the plane stress problem of an isotropic elastic plate under uniform load of value q = 100 N/mm, with zero body forces. The dimensions and boundary conditions are shown in Fig. 12. The elastic and geometrical constants are E = 210 GPa, ν = 0.3, L = 60 mm, H = 120 mm, thickness = 1 mm. The grid size is 40×81. This problem was also studied by Timoshenko and Goodier (1951), assuming normal and shear distributed forces at the ends, in according with their theoretical solution.

Figs. 13 and 14 show the network and theoretical solutions, while Table 3 gives a detail of these values at particular locations. As can be seen, the network results agree closely with the exact solution.

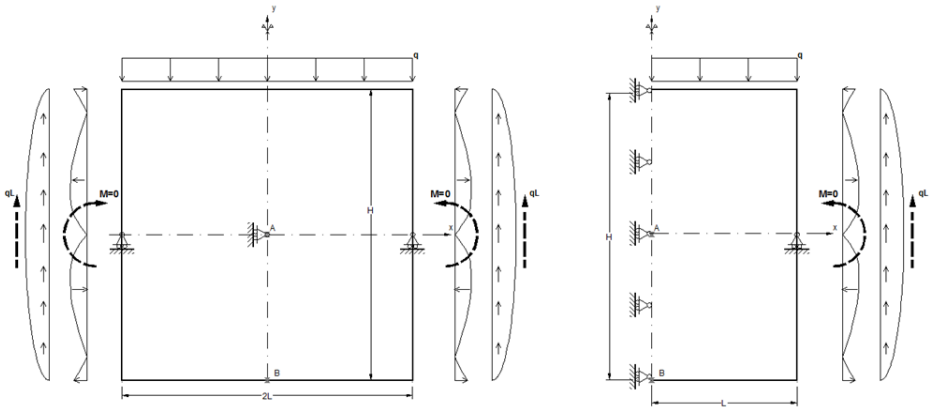

Figure 13: Geometry and boundary conditions. Left: complete model, right: symmetric model. Application 2, case a

Table 3: Comparison between network and theoretical solutions. Application 2, case a

	Theoretical	Network	Ratio	Error (%)
Point A: Deflection u_y, (mm)	-0.02929	-0.02919	0.9966	0.34
Point B: Stress σ_{xx}, (MPa)	+95.000	+95.864	1.0091	0.91

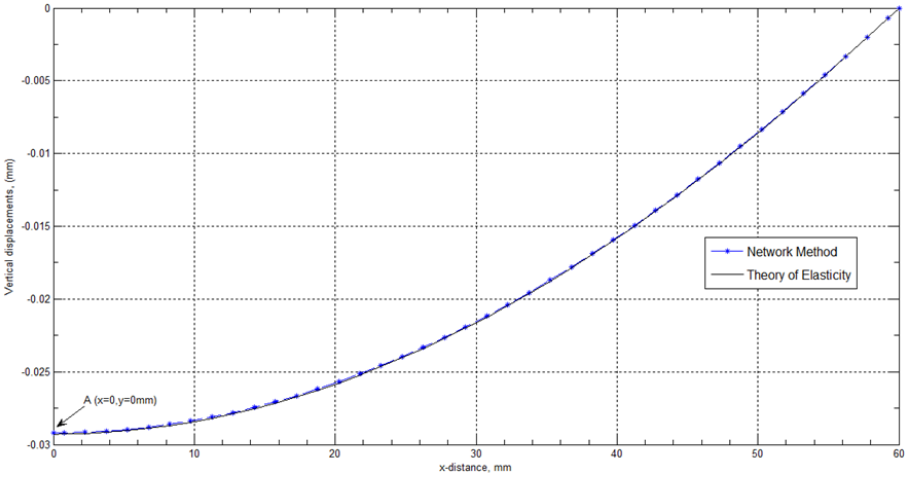

Figure 14: Vertical displacements results at y = 0. Application 2, case a

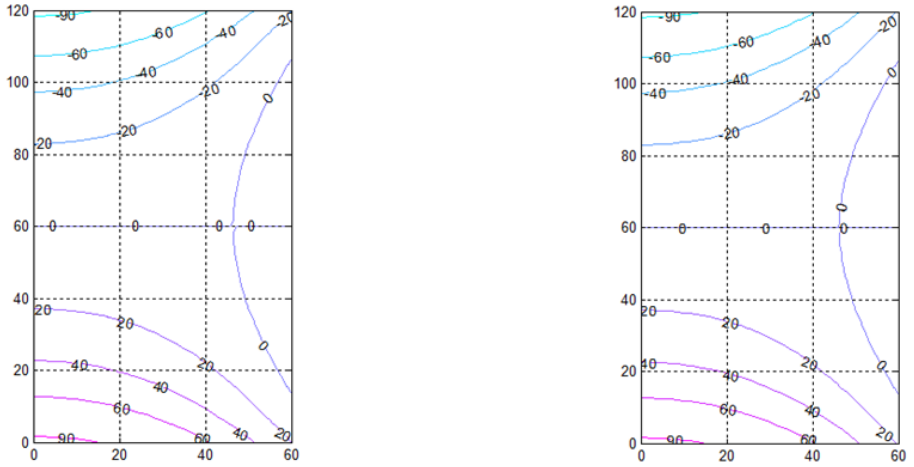

Figure 15: Displacement stress isolines σ_{xx}. Left : theoretical solution, right: network solution. Application 2, case a

4.2.2 Case b. Bending by non-uniform load

This considers the plane stress problem of an isotropic elastic plate for the case of zero body forces and q = 100 N/mm. Fig. 15 shows the geometry and boundary conditions. The geometrical parameters, material properties and grid size are sim-

ilar to these of the former case (case a). Timoshenko and Goodier (1951) solve this problem using the Airy function to illustrate the application of the difference method to the solution of 2D elastic problems.

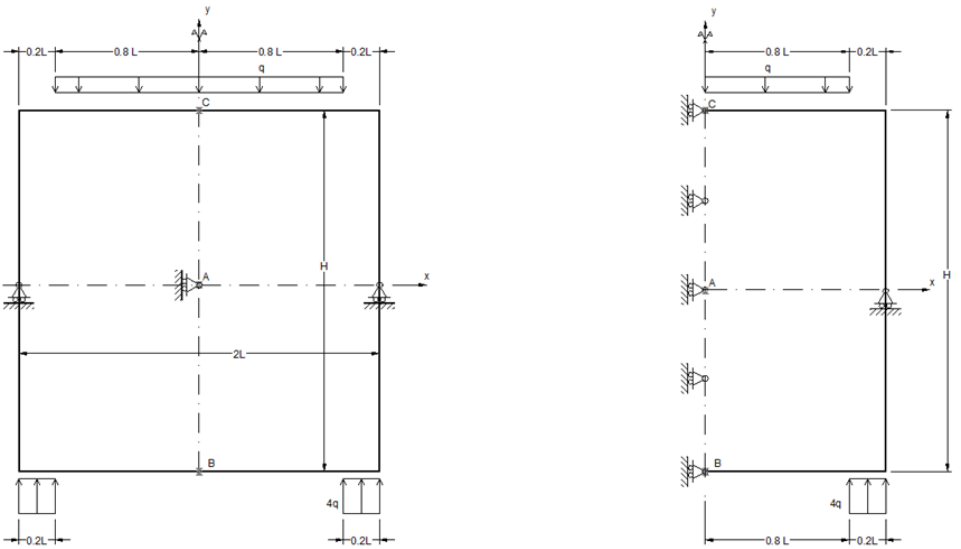

Figure 16: Geometry and boundary conditions. Left: complete model; right: symmetric model. Application2, case b

Figs. 16 and 17 show the normal stress and shear stress isolines, σ_{xx} and σ_{xy}, respectively, provided by the network and FEM solutions for comparison. For the latter, the same 2-D structural solid element as in application 1, case b [ANSYS 9.0 (2004)], and a grid size of 40×80 was used. A detail of the displacement and stress results, using five significant digits, for point A (centroid of the middle cross section) and B and C (two target points of the free surfaces), respectively, as well as their (negligible) deviations, are shown in Table 4.

Table 4: Comparison between network and FEM solutions. Application 2, case b

	FEM	Network	Ratio	Deviation(%)
Point A: Deflection $u_{y,}$ (mm)	-0.01344	-0.01345	1.0007	0.07
Point B: Stress σ_{xx}, (MPa)	+140.59	+142.24	1.0117	1.17
Point C: Stress $\sigma_{xx,}$ (MPa)	-51.99	-52.65	1.0127	1.27

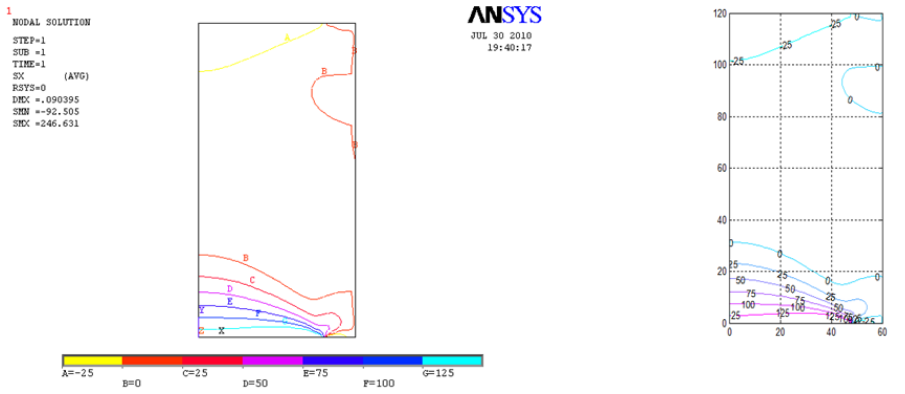

Figure 17: Normal stress isolines σ_{xx}. Left: FEM solution; right: network solution. Application 2, case b

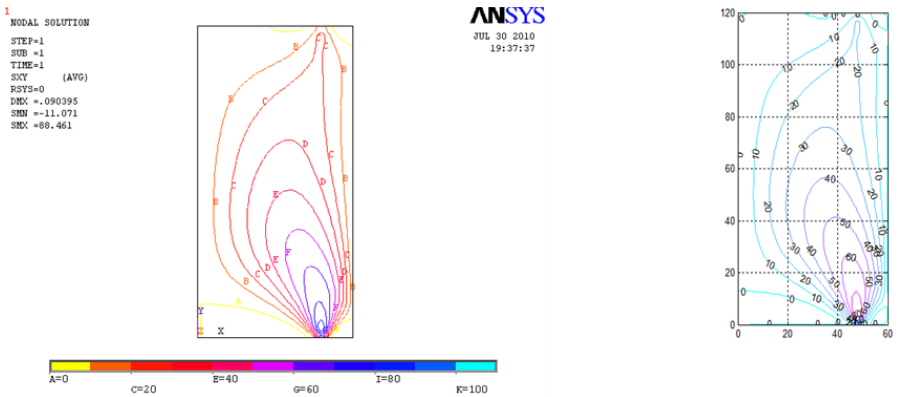

Figure 18: Shear stress isolines σ_{xy}. Left: FEM solution; right: network solution. Application 2, case b

5 Conclusions

In this work the network method has been used for the solution of linear elastostatic problems formulated by Navier's equations. After describing the design of the general purpose network model, two applications have been presented: a cantilever loaded at one end and a simply supported loaded plate. The models are simulated in a standard circuit simulation code with no other mathematical manipulations and the solution is post-processed by MATLAB for suitable graphical representation.

To demonstrate the reliability and efficiency of the method, the solutions of the proposed applications are successfully compared with those obtained analytically or numerically by a standard method. In all cases the deviations are less than 1 %.

References

ANSYS, Inc. (2004): *ANSYS Release 9.0. ANSYS, Inc., Southpointe, 275 Technology Drive, Canonsburg, PA 15317, USA.*

González Fernández, C.F. (2002): *Network Simulation Method. Ed. J. Horno, Research Signpost. Trivandrum-695023, India.*

Horno, J.; González Caballero, A.; Hayas, A.; González-Fernández, C. F. (1990): *The effect of previous convective flux on the nonstationary diffusion through membranes. J Membr Sci 48, 67-77.*

Horno, J.; Garcia Hernández, M. T.; González-Fernández, C. F. (1993): *Digital simulation of electrochemical processes by network approach. J Electroanal Chem 352, 83-97.*

Microsim Corporation (1994). *PSICE, Release 6.0. Microsim Corporation, 20 Fairbanks, Irvine, California 92718.*

Moreno Nicolás, J. A.; Gómez de León Hyjes; Alhama, F. (2007): *Solution of temperature fields in hydrodynamics bearing by the numerical network model. Tribology International 40, 139-145.*

Nagel, L.W. (1977): *SPICE, Simulation program with integrated circuit emphasis. Berkeley, CA, University of California, Electronic Res. Lab., ERL-M382.*

Sadd, M. H. (2009): *Elasticity. Theory, Applications, and Numerics, second ed., Academic Press/Elsevier.*

Soto Meca, A.; Alhama, F.; González-Fernández, C. F. (2007): *An efficient model for solving density driven groundwater flow problems based on the network simulation method. Journal of Hidrology 339, 39-53.*

Timoshenko, S.; Goodier, J. N. (1951): *Theory of Elasticity, second ed., McGraw-Hill.*

Zueco, J.; Alhama, F. (2007): *Simultaneous inverse determination of temperature-dependent thermophysical properties in fluids using the network simulation method. Int J Heat Mass Transf 50, 3234-3243.*